

Article

Not peer-reviewed version

---

# Raman Spectroscopic and Surface-Enhanced Raman Spectroscopic Analyses of Normal Blood and Abnormal Blood

---

[Song-Jeng Huang](#)<sup>\*</sup>, Jun-Han Lan, [Chao-Ching Chiang](#), [Fang-Yuh Lo](#)<sup>\*</sup>, [Kung-Chia Young](#)<sup>\*</sup>

Posted Date: 2 May 2023

doi: 10.20944/preprints202305.0053.v1

Keywords: blood testing, biological information; hemoglobin; Raman spectroscopy; surface-enhanced Raman spectroscopy (SERS)



Preprints.org is a free multidiscipline platform providing preprint service that is dedicated to making early versions of research outputs permanently available and citable. Preprints posted at Preprints.org appear in Web of Science, Crossref, Google Scholar, Scilit, Europe PMC.

Copyright: This is an open access article distributed under the Creative Commons Attribution License which permits unrestricted use, distribution, and reproduction in any medium, provided the original work is properly cited.

## Article

# Raman Spectroscopic and Surface-Enhanced Raman Spectroscopic Analyses of Normal Blood and Abnormal Blood

Song-Jeng Huang <sup>1,\*</sup>, Jun-Han Lan <sup>1</sup>, Chao-Ching Chiang <sup>1</sup>, Fang-Yuh Lo <sup>2,\*</sup>  
and Kung-Chia Young <sup>3,\*</sup>

<sup>1</sup> Department of Mechanical Engineering, National Taiwan University of Science and Technology;

<sup>2</sup> Department of Physics, National Taiwan Normal University;

<sup>3</sup> Department of Medical Laboratory Science and Biotechnology, National Cheng Kung University;

\* Correspondence: sgjhuang@mail.ntust.edu.tw (S-J H) fangyuhlo@ntnu.edu.tw (F-Y L)  
t7908077@ncku.edu.tw (K-C Y);

**Abstract:** Blood testing is a crucial medical application. In this study, we applied Raman spectroscopy to test blood samples and obtained complete biological information, including the main components and compositions in these samples. Short-wavelength (532-nm green light) Raman scattering spectroscopy was conducted on samples of normal blood, abnormal blood in 3 types of preparation including whole blood, plasma, and serum, and the underlying information reflected by the biological characteristics detected in each sample type were analyzed. Raman spectroscopy results indicated that normal blood had high hemoglobin content, which suggests that hemoglobin is a major component of blood. Hemoglobin affects blood oxygen level. The characteristic peaks of hemoglobin were observed at 690, 989, 1015, 1182, 1233, 1315, and 1562–1649  $\text{cm}^{-1}$ . Analysis of plasma and serum samples indicated the presence of  $\beta$ -carotene, which exhibited characteristic peaks at 1013, 1172, and 1526  $\text{cm}^{-1}$ . In addition, surface-enhanced Raman spectroscopy was used to collect biological signals that are difficult to obtain in conventional Raman spectroscopy, including those of small molecules such as hormones, antibodies, and enzymes. Changes in biological information collected in this manner can be used as a basis for potentially diagnosing clinical diseases.

**Keywords:** blood testing; biological information; hemoglobin; Raman spectroscopy; surface-enhanced Raman spectroscopy (SERS)

## 1. Introduction

Conventional blood tests are observed with optical microscopes. These tests are time-consuming and can reduce the integrity of blood samples. Among the emerging laser-based methods for blood testing, Raman spectroscopy is one of the methods that involves nonlinear scattering. This method is adopted in a wide range of blood tests because of its various advantages, such as the requirement of only a minimal quantity of blood for testing, rapid analysis, and high-precision result interpretation, which simplify the collection and assessment of blood-related data. The effectiveness of Raman spectroscopy in clinical applications has been verified [1,2].

In Raman spectroscopy, the wavelength difference between incident and scattered light is compared to determine the changes in their energy levels and the sample's lattice vibration characteristics, both of which can be used to analyze the composition and structure of the sample. Therefore, the values of Raman peaks can indicate the molecular structure of a sample [3,4].

Raman **scattering** spectroscopy can be applied with blood testing to determine if an individual has contracted a certain disease. The Raman **characteristic peak positions** and amplitudes of an infected individual differ markedly from those of an uninfected individual. Thus, Raman spectroscopy can enable rapid screening for certain pathogens. The prevalence of emerging viruses, such as COVID-19, will eventually be overlapped to that of influenza virus infection, and this trend has necessitated reliable and rapid and differential disease screening [5]. Moreover, the acquisition of blood information through Raman spectroscopy enables the rapid and precise diagnosis of clinical

diseases, such as liver disease, diabetes, cancer, allergies, genetic disorders, anemia, and leukemia [6–8].

In the present study, Raman spectroscopy was employed to analyze samples of normal blood and abnormal blood, in 3 types of preparation, including whole blood, plasma, and serum. The primary Raman peaks of normal blood was observed to correspond to hemoglobin, and the other Raman peaks of normal blood corresponded to amino acid and other components [9]. By contrast, the primary Raman peaks of plasma and serum corresponded to  $\beta$ -carotene [10]. We also conducted surface-enhanced Raman spectroscopy (SERS) to examine the small molecules present in the aforementioned samples. Moreover, a prothrombin time experiment was performed to compare the Raman spectroscopy results of blood samples with and without calcium-containing coagulants. Clinically, coagulation or clotting, in which blood turns from liquid to nonflowing gel, is a critical process in hemostasis [11,12]. **The goal was to determine whether patients' intrinsic and common coagulation pathways were functioning normally.**

## 2. Sample Preparation

All blood samples used in this study were obtained from the waste blood provided by National Cheng Kung University Hospital with the approval of its institutional review board. Three-types of sample preparation were collected for each blood specimen. None of the normal samples used in this study were subjected to any chemical or biological treatment. Blood samples were drawn using a syringe, dropped on a glass slide (100  $\mu$ L), and then covered with a cover glass. An experiment was conducted on the blood samples at room temperature. Normal blood, which was obtained from healthy individuals, typically had a prothrombin time of 10.0–12.5 s. By comparison, abnormal blood, which was obtained from patients receiving anticoagulant drugs, had a clotting time of longer than 12.5 s. For experimental protocol, a calcium-containing coagulant had to be mixed with blood in a ratio of 2.8:1, and silver nanoparticles were mixed with the blood samples in a ratio of 1:3. To meet the requirements of clinical practice, the prepared whole blood and plasma samples were also examined.

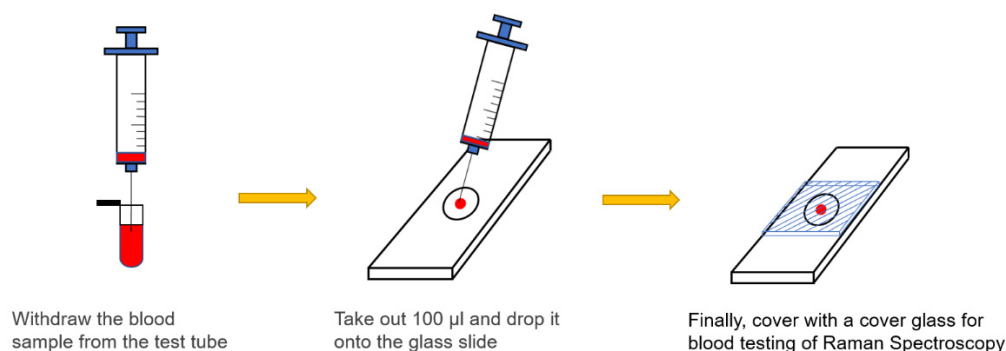


**Figure 1.** Preparation of blood samples.

## 3. Raman spectroscopy

Raman scattering spectroscopy and surface-enhanced Raman spectroscopy (SERS) were performed at room temperature (RT) using a custom-made micro-Raman spectroscopy system consisting of a spectrometer (Princeton Instruments Acton Spectra Pro 2500i), a liquid nitrogen cooled CCD detector (Princeton Instruments Acton 7508-0002), four objective lenses from 20x to 100x, and a solid-state green laser (wavelength of 532 nm) as its excitation light source. To avoid laser heating damage of blood samples, each Raman scattering spectrum was recorded with the integration of 3 s for 5 times for the laser output power of 3 mW and the 20x objective lens. The spectral range was set between 400 and 2000  $\text{cm}^{-1}$ . The blood samples were contained on a glass slide sealed with a cover glass, and for SERS, the blood samples were mixed with Ag nanoparticles. All spectra were recorded

a few minutes after each sample was made. The Raman characteristic peak position was calibrated with measurements of a Si(100) substrate under the same conditions, and the background intensity was subtracted. In addition, the Raman spectra is normalized to the characteristic peak of normal blood at 1562 cm<sup>-1</sup>, and the SERS spectra is normalized to the characteristic peak of normal blood at 521 cm<sup>-1</sup>.

4. Results and discussion

4.1. Raman spectrum for normal blood

On the basis of a literature review and matching inquiries in the Spectral Database for Organic Compounds [13] we found that the most abundant component in normal whole blood is hemoglobin [14], followed by amino acid, lactic acid, lactate, and acetate. Hemoglobin, which is a major component of whole blood, were observed to exhibit characteristic peaks at 690, 989, 1015, 1182, 1233, 1315, and 1562–1649 cm<sup>-1</sup>. Hemoglobin accounts for 95% of the weight of a red blood cell and affects a red blood cell’s oxygen carrying capacity [15]. In clinical practice, hemoglobin level can serve as a standard for anemia detection [16], and the severity of COVID-19 disease can be predicted using blood oxygen level [5]. Amino acid is small molecule [17] which exhibited characteristic peaks at 770 and 1348 cm<sup>-1</sup>. Moreover, lactic acid and lactate exhibited characteristic peaks at 1092 and 1144 cm<sup>-1</sup>, respectively. Lactic acid is a metabolic product of carbohydrate, and blood lactic acid level can serve as a standard for the diagnosis of lactic acidosis in clinical practice [18]. Lactate is a salt formed through the release of a hydron from lactic acid after lactic acid reacts with a charge-carrying sodium or potassium ion. An excessive lactate level is recognized as a potential cause for acidemia (acidosis) [19]. The main characteristic peak of acetate was located at 1441 cm<sup>-1</sup>. Acetate exists in animal tissues, excreta, and blood in the form of free acid (Figure 2). Table 1 presents the Raman peaks and vibrational modes of the components of normal blood [20].

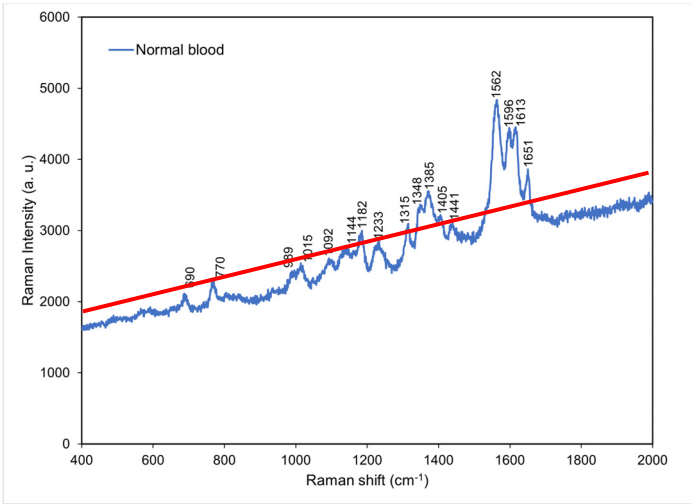


**Figure 2.** Raman spectrum obtained for normal blood at room temperature. The red solid line indicates the background of the spectrum.

**Table 1.** Characteristic peaks and **corresponding** vibrational modes of the components of normal blood.

Raman shift (cm <sup>-1</sup> )	Vibrational mode	Component
690	C-C-N bending	Hemoglobin
770	Ring vibrations	Tryptophan
989	Aromatic ring breathing	Hemoglobin
1015	Aromatic ring breathing	Hemoglobin
1092	C-O vibrations	Lactic acid

1144	CH <sub>3</sub> rocking, C-O vibrations	Lactate
1182	C-C stretching	Hemoglobin
1233	Ferrous low spin	Hemoglobin
1315	C-C stretching	Hemoglobin
1348	C-H bending	Tryptophan
1385	CH <sub>3</sub> symmetric stretching	Heme
1405	C=N antisymmetric stretching	Heme
1441	CH <sub>2</sub> bending	Acetates
1562	Pyrrole ring stretching vibrations	Hemoglobin
1596	C=N antisymmetric stretching and	Hemoglobin
1613	C-H bending	Hemoglobin
1651	Ferrous low spin	Hemoglobin

#### 4.2. Comparison of the Raman spectra of normal blood and abnormal blood

According to Figure 3, the greatest difference in the Raman spectra of normal blood and abnormal blood occurred between 1562 and 1651 cm<sup>-1</sup>. The normal sample exhibited characteristic peaks at 1562 and 1613 cm<sup>-1</sup>, whereas the abnormal sample exhibited a characteristic peak at 1574 cm<sup>-1</sup>. This result suggests that the coagulation of hemoglobin was easier in normal blood than in abnormal blood because of the shorter time period for clotting of normal blood. Accordingly, the characteristic peaks of aromatic ring breathing, **C=N antisymmetric stretching**, and pyrrole ring stretching were **either absent or shifted in peak position in the abnormal blood Raman spectrum**. Table 2 presents the major Raman shifts and corresponding components for normal whole blood and abnormal whole blood [21].

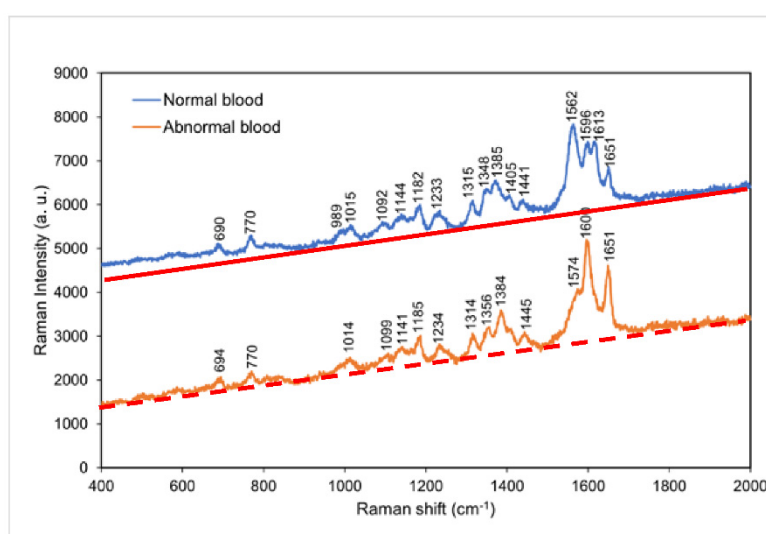


**Figure 3.** Raman spectra of normal blood and abnormal blood at room temperature. The red solid line and orange dashed line indicate the background for each spectrum, respectively.

**Table 2.** Major Raman shifts and corresponding components for normal blood and abnormal blood.

Normal Raman shift (cm <sup>-1</sup> )	Abnormal blood Raman shift (cm <sup>-1</sup> )	Vibrational blood mode	Component
989	No	Aromatic ring breathing	Hemoglobin
1315	1314	C-C stretching	Hemoglobin
1348	1356	C-H bending	Tryptophan
1562	1574	Pyrrole ring stretching vibrations	Hemoglobin
1596	1600	C=N antisymmetric stretching	Hemoglobin

1613	No	C-H bending	Hemoglobin
1651	1651	Ferrous low spin	Hemoglobin

4.3. Comparison of the Raman spectra of normal blood with and without coagulant

Figure 4 compares the Raman spectra of normal blood with and without coagulant. Normal blood with coagulant has lower intensities at the characteristic peaks of 769, 987, 1014, 1315, 1352, and 1565  $\text{cm}^{-1}$  and higher intensities at the characteristic peaks of 1598 and 1649  $\text{cm}^{-1}$ . This result suggests that hemoglobin was considerably affected by clotting process [22,23] and that an excessively short time period of clotting resulted in incomplete coagulation. This led to incomplete molecular reactions in the blood and thus a decrease in the intensities of some characteristic peaks. Table 3 presents the major Raman shifts and corresponding components for normal blood with and without coagulant.

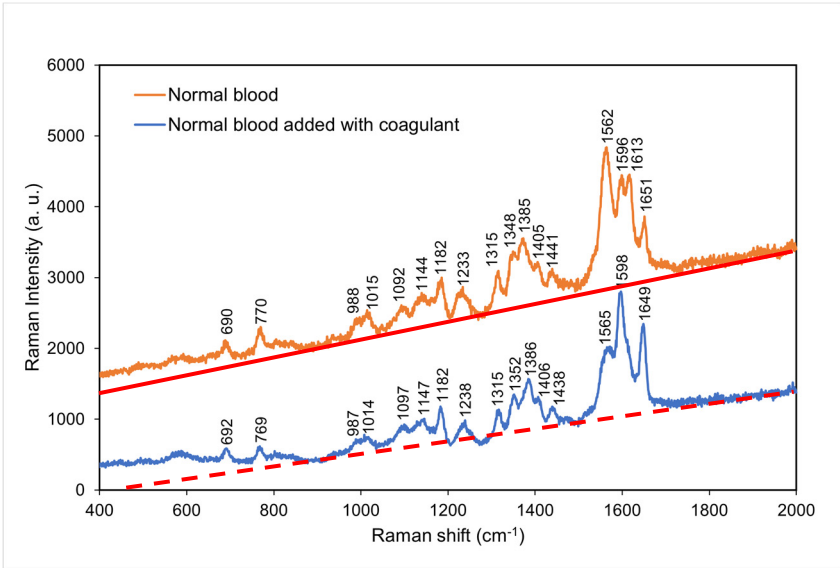


**Figure 4.** Raman spectra of normal blood with and without coagulant at room temperature. The red solid line and orange dashed line indicate the background for each spectrum, respectively.

**Table 3.** Major Raman shifts and corresponding components for normal blood with and without coagulant.

Normal blood Raman shift ( $\text{cm}^{-1}$ )	Normal blood (Coagulant) Raman shift ( $\text{cm}^{-1}$ )	Vibrational mode	Component
770	769	Ring vibrations	Tryptophan
988	987	Aromatic ring breathing	Hemoglobin
1015	1014	Aromatic ring breathing	Hemoglobin
1315	1315	C-C stretching	Hemoglobin
1348	1352	C-H bending	Tryptophan
1562	1565	Pyrrole ring stretching vibrations	Hemoglobin
1596	1598	C=N antisymmetric stretching	Hemoglobin
1613	No	C-H bending	Hemoglobin
1651	1649	Ferrous low spin	Hemoglobin



4.4. Comparison of the Raman spectra of abnormal blood with and without coagulant

According to Figure 5, **the comparison between abnormal blood with and without coagulant, the abnormal blood with coagulant had lower intensities at the characteristic peaks of 770, 1011, 1185, 1318, 1356, 1384, and 1712 cm<sup>-1</sup> and higher intensities at the characteristic peaks of 988 and 1577 cm<sup>-1</sup>. Such change in intensity without shift in peak position is attributed to (significant) change in clotting time of hemoglobin. The addition of coagulant shortens the clotting time, and therefore, the abnormal blood, originally having a long time period of clotting, became fully coagulated after the addition of coagulant.** Table 4 presents the major Raman shifts and corresponding components for normal blood without coagulant and abnormal blood with coagulant.

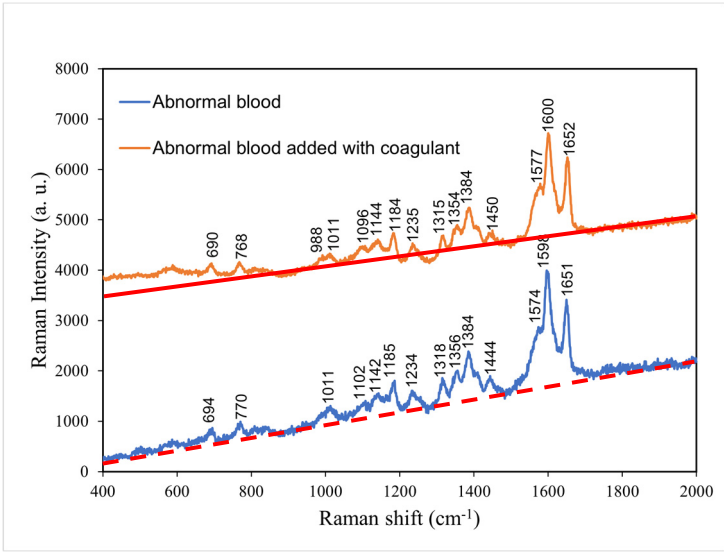


**Figure 5.** Raman spectra of normal blood without coagulant and abnormal blood with coagulant at room temperature. The red solid line and orange dashed line indicate the background for each spectrum, respectively.

**Table 4.** Major Raman shifts and corresponding components for **abnormal blood with and without coagulant.**

Abnormal blood Raman shift (cm <sup>-1</sup> )	Abnormal blood (Coagulant) Raman shift (cm <sup>-1</sup> )	Vibrational mode	Component
770	768	Ring vibrations	Tryptophan
1185	1184	C-C stretching	Hemoglobin
1318	1315	C-C stretching	Hemoglobin
1356	1354	C-H bending	Tryptophan
1574	1577	Pyrrole ring stretching vibrations	Hemoglobin

4.5. Comparison of the Raman spectra of normal blood with coagulant and abnormal blood with coagulant

According to Figure 6, the characteristic peaks of abnormal blood with coagulant were similar to those of normal blood with coagulant. Thus, the addition of coagulant to abnormal blood resulted in the locations and intensities of its characteristic peaks ~~gradually~~ approaching those of the characteristic peaks of normal blood with coagulant. **This indicated that the coagulation cascades were commonly shared in individuals with either normal or abnormal blood samples, but the required time periods for full coagulation differed.** In addition, the presence of coagulant effectively shortened the time period of clotting of abnormal blood and caused full coagulation.

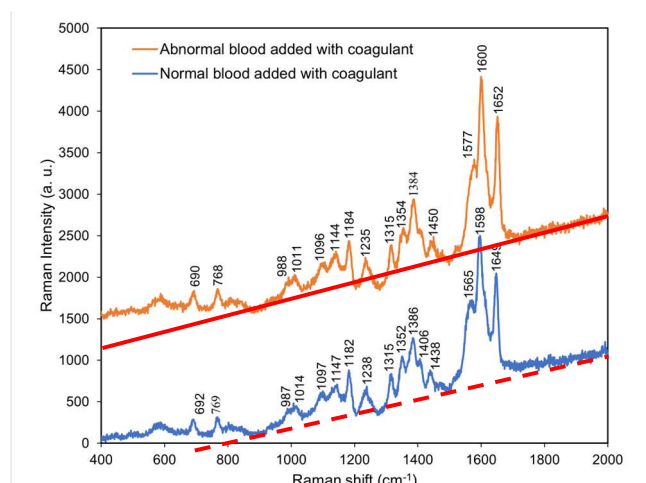


**Figure 6.** Raman spectra of normal blood with coagulant and abnormal blood with coagulant at room temperature. The red solid line and orange dashed line indicate the background for each spectrum, respectively.

#### 4.6. Comparison of the normal and surface-enhanced Raman spectra of normal blood without coagulant

The surface-enhanced Raman spectrum was mainly conducted to reinforce Raman spectrum at low frequency because molecular resonance at a low frequency can be achieved more easily in SERS than in Raman spectroscopy. Therefore, in Figure 7, molecular vibration modes at high frequencies have higher intensity while in SERS, low frequency vibration modes are stronger [24]. In the low frequency region, SERS peaks at 400–1000  $\text{cm}^{-1}$  revealed considerable additional biological information that could not be obtained through normal Raman spectroscopy, including the presence of hormone, antibody, and enzyme molecules from 440.  $\text{cm}^{-1}$  to 797  $\text{cm}^{-1}$ . Above 1000  $\text{cm}^{-1}$ , SERS spectrum does not reveal additional biological characteristics than that of Raman spectroscopy. Table 5 presents the major Raman shifts in the normal and surface-enhanced Raman spectra of normal blood without coagulant and the components corresponding to these shifts [24].

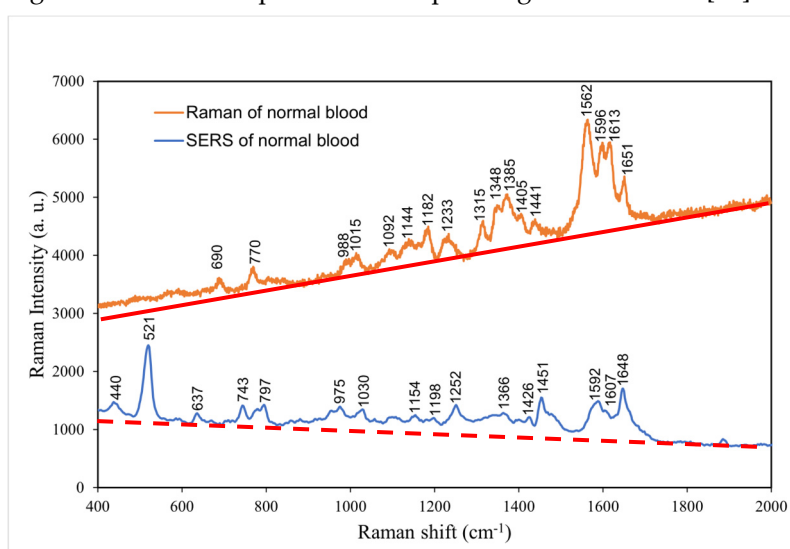


**Figure 7.** Normal and surface-enhanced Raman spectra of normal blood without coagulant at room temperature. The red solid line and orange dashed line indicate the background for each spectrum, respectively.



**Table 5.** Major Raman shifts in the normal and surface-enhanced Raman spectra of normal blood without coagulant and the components corresponding to these shifts.

Normal Raman shift (cm <sup>-1</sup> )	Normal blood (SERS) Raman shift (cm <sup>-1</sup> )	Vibrational blood mode	Component
No	440	C-C-N bending	L-Arginine
No	521	S-S disulfide stretching in Proteins	Cholesterol ester
No	637	C-C-N bending	Tyrosine
No	743	C-H bending	Coenzyme A
No	797	Ring vibrations	L-Serine
No	975	Aromatic ring breathing	Phenylalanine
1015	1030	Aromatic ring breathing	Hemoglobin
No	1154	CH3 rocking, C-O vibrations	D-mannos
1182	1198	C-C stretching	L-tryptophan
1233	1252	Ferrous low spin	Hemoglobin
1348	1366	CH3 symmetric stretching	Heme
1405	1426	C=N antisymmetric stretching	Heme
1441	1451	CH2 bending	Acetates
1596	1592	C=N antisymmetric stretching	Hemoglobin
1613	1607	C-H bending	Hemoglobin
1651	1648	Ferrous low spin	Hemoglobin

4.7. Comparison of the normal and surface-enhanced Raman spectra of abnormal blood without coagulant

According to Figure 8, the surface-enhanced Raman spectrum of abnormal blood without coagulant exhibited additional peaks at 400–800 and 1600–2000 cm<sup>-1</sup> (low- and high-frequency regions, respectively) that were not observed in the normal Raman spectrum of abnormal blood without coagulant. However, the surface-enhanced Raman spectrum exhibited considerably fewer peaks in the mid-frequency region of 700–1600 cm<sup>-1</sup> than did the normal Raman spectrum. **Comparing the SERS spectra of normal and abnormal blood at the low frequency part, the Coenzyme A characteristic peak (743 cm<sup>-1</sup>) is missing in the abnormal blood, and characteristic peak positions of L-Arginine, Cholesterol ester, and Phenylalanine shift significantly. This indicates that the abnormal blood environment probably leads to change in bond lengths in L-Arginine, Cholesterol ester, and Phenylalanine molecules.** Overall, the SERS results of abnormal blood without coagulant differed from those of normal blood without coagulant (Figure 7), **and the strong difference at low frequency vibration modes can serve as fingerprints for diagnostics.** Table 6 presents the major Raman shifts in the normal and surface-enhanced Raman spectra of abnormal blood without coagulant and the components corresponding to these shifts [25].

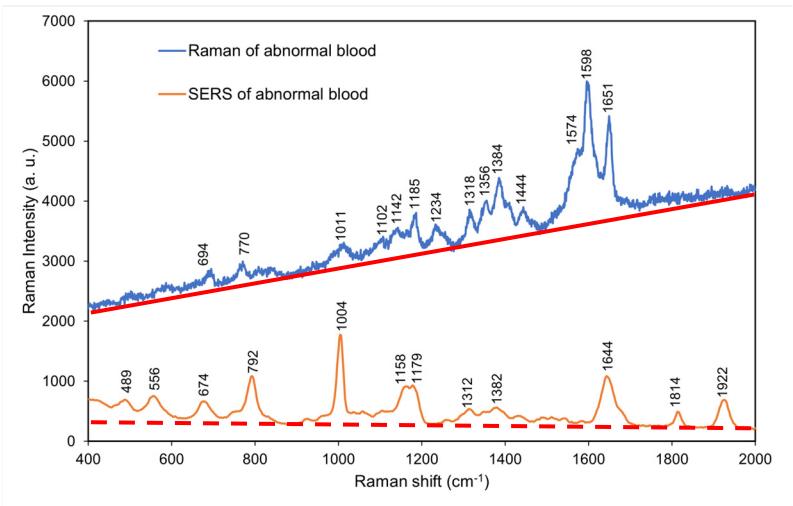


**Figure 8.** Normal and surface-enhanced Raman spectra of abnormal blood without coagulant at room temperature. The red solid line and orange dashed line indicate the background for each spectrum, respectively.

**Table 6.** Major Raman shifts in the normal and surface-enhanced Raman spectra of abnormal blood without coagulant and the components corresponding to these shifts.

Abnormal blood Raman shift (cm <sup>-1</sup> )	Abnormal blood (SERS) Raman shift (cm <sup>-1</sup> )	Vibrational blood mode	Component
No	489	C-C-N bending	L-Arginine
No	556	S-S disulfide stretching in Proteins	Cholesterol ester
No	674	C-C-N bending	Tyrosine
No	792	Ring vibrations	L-Serine
1011	1004	Aromatic ring breathing	Phenylalanine
1142	1158	CH3 rocking, C-O vibrations	Lactate
1185	1179	C-C stretching	Hemoglobin
1318	1312	CH3CH2 twisting	Collagen
1384	1382	C-C stretching	L-tryptophan
1648	1644	Ferrous low spin	Hemoglobin
No	1814	Aromatic ring breathing	Hemoglobin
No	1922	Ring vibrations	Hemoglobin

4.8. Comparison of the Raman spectra of whole blood, plasma, and serum

**The whole blood is the** normal blood that contains anticoagulant to inhibit coagulation. The characteristic peaks of whole blood had lower intensities than those of normal blood because of the lack of coagulation in whole blood, which resulted in its molecules being unable to achieve resonance. However, the overall waveforms obtained for normal blood and whole blood were similar (Figure 9). By contrast, plasma and serum exhibited characteristic peaks only at 1016, 1153, and 1526 cm<sup>-1</sup> because only some small molecules remained after the removal of blood cells. A study suggested that the characteristic peaks of plasma and serum correspond to β-carotene [26], which only exhibits molecular resonance at low frequencies. In clinical application, changes in the characteristic β-carotene peaks in the Raman spectra of serum and plasma can be used to diagnose certain diseases, such as thyroid disease and chronic renal failure. Researchers have recommended using the Raman shift of β-carotene for diagnosing chronic renal failure and thyroid disease [27]. Tables 7–9 present the major Raman shifts and corresponding components for whole blood [19], plasma [27], and serum [28].

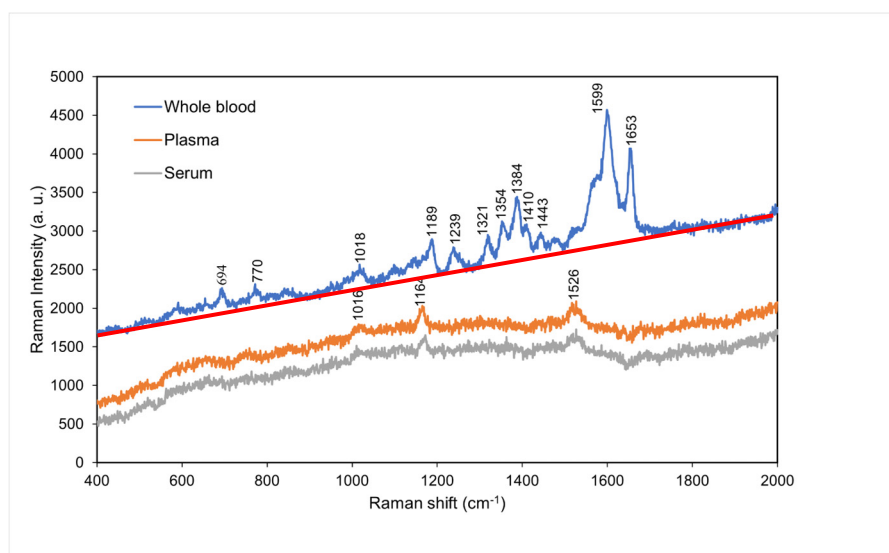


**Figure 9.** Raman spectra of whole blood, plasma, and serum at room temperature. The red solid line indicates the background of the spectrum for whole blood.

**Table 7.** Major Raman shifts and corresponding components for whole blood.

Raman shift (cm <sup>-1</sup> )	Vibrational blood mode	Component
694	C-C-N bending	Hemoglobin
770	Ring vibrations	Tryptophan
1018	Aromatic ring breathing	Hemoglobin
1189	C-C stretching	Hemoglobin
1239	Ferrous low spin	Hemoglobin
1321	C-C stretching	Hemoglobin
1354	C-H bending	Tryptophan
1384	CH <sub>3</sub> symmetric stretch	Heme
1410	C=N antisymmetric stretching	Heme
1443	CH <sub>2</sub> bending	Acetates
1599	C-H bending	Hemoglobin
1653	Ferrous low spin	Hemoglobin

**Table 8.** Major Raman shifts and corresponding components for plasma.

Raman shift (cm <sup>-1</sup> )	Vibrational blood mode	Component
1016	C-H bending	β-Carotene
1164	C-C stretching	β-Carotene
1526	C-C stretching	β-Carotene

**Table 9.** Major Raman shifts and corresponding components for serum [28].

Raman shift (cm <sup>-1</sup> )	Vibrational blood mode	Component
1013	C-H bending	β-Carotene
1172	C-C stretching	β-Carotene
1526	C-C stretching	β-Carotene

## 5. Conclusions

Using short-wavelength Raman scattering spectroscopy and SERS, samples of normal blood, abnormal blood in whole blood, plasma, and serum were detected, and the underlying information reflected by the biological characteristics detected in each sample type were analyzed. As a result of the analysis, the following major conclusions and new finding were reached:

1. The addition of coagulant effectively and gradually caused the intensities and locations of the characteristic peaks of abnormal blood to approach those of the characteristic peaks of normal blood with coagulant, which indicates that the blood clotting affects the locations and intensities of characteristic peaks caused by hemoglobin.
2. The SERS results of abnormal blood without coagulant differed from those of normal blood without coagulant, **and the strong difference at low frequency vibration modes can serve as fingerprints for diagnostics.**
3. In serum and plasma, the main molecule that resonates in Raman spectroscopy excludes hemoglobin, but  $\beta$ -carotene only exhibits molecular resonance at low frequencies. Therefore,  $\beta$ -carotene might become crucial component in medical testing.

**Acknowledgments:** The authors thank the Ministry of Science and Technology, Taiwan, Republic of China (contract numbers: MOST 109-2224-E-011 -002), for supporting the research and publication

## References

1. Kong, K.; Kendall, C.; Stone, N.; Notingher, I. Raman spectroscopy for medical diagnostics — From in-vitro biofluid assays to in-vivo cancer detection. *Volume*. **2015**, 89, 121-134. <https://doi.org/10.1016/j.addr.2015.03.009>.
2. Pence, I.J.; Janse, A.M.- Clinical instrumentation and applications of Raman spectroscopy. *Chem. Soc. Rev.* **2016**, 45, 1958–1979. <https://doi.org/10.1039/c5cs00581g>.
3. Workman, J. Infrared and Raman spectroscopy in paper and pulp analysis. *Appl. Spectrosc. Rev.* **2001**, 36, 139-168. <https://doi.org/10.1081/ASR-100106154>.
4. Sil, S.; Umapathy, S. Raman spectroscopy explores molecular structural signatures of hidden materials in depth: Universal Multiple Angle Raman Spectroscopy. *Sci. Rep.* **2014**, 4, 5308. <https://doi.org/10.1038/srep05308>.
5. Ganesh, K.V.S.S.; Bevi, A.R. Low-Cost Pulse Oximeter & Heart Rate Measurement for COVID Diagnosis. *J. Phys.: Conf. Ser.* **2021**, 1964, 62035. <https://doi.org/10.1088/1742-6596/1964/6/062035>.
6. Han, H.W.; Yan, X.L.; Dong, R.X.; Ban, G.; Li, K. Analysis of serum from type II diabetes mellitus and diabetic complication using surface-enhanced Raman spectra (SERS). *Appl. Phys.* **2009**, 94, 667-672. <https://doi.org/10.1007/s00340-008-3299-5>.
7. Rusciano, G.; Luca, A.C.D.; Pesce, G.; Sasso, A. Raman Tweezers as a Diagnostic Tool of Hemoglobin-Related Blood Disorders. *Sensor*. **2008**, 8, 7818–7832. <https://doi.org/10.3390/s8127818>.
8. Han, H.; Gong, j.; Tian, Y. Analysis of Serum from Acute Leukemia Patients Using Surface-Enhanced Raman Spectroscopy (SERS). *Spectroscopy*, **2022**, 37, 36-41.
9. Atkins, C.G.; Buckley, K.; Blades, M.W.; Turner, R.F.B. Raman Spectroscopy of Blood and Blood Components. *Appl. Spectrosc.* **2017**, 71, 767-793. <https://doi.org/10.1177/0003702816686593>.
10. Albanes, D.  $\beta$ -Carotene and lung cancer: a case study. *Volume*. **1999**, 69, 1345-1350. <https://doi.org/10.1093/ajcn/69.6.1345S>.
11. Huang, S.J.; Chiang, C.C.; Immanue, P.N.; Subramania M. Point-of-Care Testing Blood Coagulation Detectors Using a Bio-Microfluidic Device Accompanied by Raman Spectroscopy. *Coatings* **2022**, 12, 893. <https://doi.org/10.3390/coatings12070893>.
12. Staritzbichler, R.; Hunold, P.; Lopis, I.E.-; Hildebrand, P.W.; Isermann, B.; Kaiser, T. Raman spectroscopy on blood serum samples of patients with end-stage liver disease. *PLoS One*. **2021**, 16, 256045. <https://doi.org/10.1371/journal.pone.0256045>. eCollection 2021.
13. Sansano, A.; Navarro, R.; Arranz, A.S.; Manrique, J.A. Development of a Spectral Data Base for Exomars' Raman Instrument (RLS). *LPSC*. **2014**, 45, 2803.
14. Enejder, A.M.; Koo, T.W.; Oh, J.; Hunter, M.; Sasic, S.; Feld, M. S.; Horowitz, G.L. Blood analysis by Raman spectroscopy. *Optics letters*. **2002**, 27, 2004-2006. <https://doi.org/10.1364/OL.27.002004>.
15. Filho, I.T.; Turner, J.; Pittman, R.N.; Somera, S.G. The Effect of Red Blood Cell Velocity on Oxygenation Measurements using Resonance Raman Spectroscopy. *Am J Physiol Heart Circ Physiol*. **2005**, 289, 488-495. <https://doi.org/10.1152/ajpheart.01171.2004>.
16. Miller, J.L. Iron Deficiency Anemia: A Common and Curable Disease. *Cold Spring Harb Perspect Med*. **2013**, 3, 11866. <https://doi.org/10.1101/cshperspect.a011866>.
17. Friedman, M. Analysis, Nutrition, and Health Benefits of Tryptophan. *Int J Tryptophan Res.* **2018**, 11, 1178646918802282. <https://doi.org/10.1177/1178646918802282>.
18. Brooks, G.A. Current concepts in lactate exchange. *Med. Sci. Sports. Exerc.* **1991**, 23, 895-906. <https://doi.org/10.1249/00005768-199004000-00003>.
19. Cairns, S.P. Lactic Acid and Exercise Performance. *Sports Med.* **2006**, 36, 279-291. <https://doi.org/10.2165/00007256-200636040-00001>.

20. Ahlawat, S.; Kumar, N.; Uppal, A.; Gupta, P.K. Visible Raman excitation laser induced power and exposure dependent effects in red blood cells. *J of Biophotonics*. **2016**, *10*, 1–8. <https://doi.org/10.1002/jbio.201500325>.
21. Bankapur, A.; Zachariah, E.; Chidangil, S.; Valiathan, M.; Mathur, D. Raman Tweezers Spectroscopy of Live, Single Red and White Blood Cells. *PLoS ONE*. **2010**, *5*, 10407. <https://doi.org/10.1371/journal.pone.0010427>.
22. Yang, C.L.; Chiou, Y.C.; Chou, C.W.; Young, K.C.; Huang, S.J.; Liu, C.Y. Point-of-care Testing Portable Blood Coagulation Detectors Using Optical Sensors. *Journal of Medical and Biological Engineering*. **2013**, *33*, 319–324.
23. Yang, C.L.; Huang, S.J.; Chou, C.W.; Chiou, Y.C.; Lin, K.P.; Tsai, M.S.; Young, K.C. Design and evaluation of a portable optical-based biosensor for testing whole blood prothrombin time. *Talanta*. **2013**, *116*, 704–711.
24. Li, H.; Wang, Q.; Tang, J.; Gao, N.; Yue, X.; Wang, T. Establishment of a reliable scheme for obtaining highly stable SERS signal of biological serum. *Biosens. Bioelectron.* **2021**, *189*, 113315. <https://doi.org/10.1016/j.bios.2021.113315>.
25. Lin, H.; Zhou, J.; Wu, Q.; Hung, T.M.; Chen, W.; Yu, Y.; Chang, J.T.C.; Pan, J.; Qiu, S.; Chen, R. Human blood test based on surface-enhanced Raman spectroscopy technology using different excitation light for nasopharyngeal cancer detection. *IET Nanobiotechnology*. **2019**, *13*, 942–945. <https://doi.org/10.1049/iet-nbt.2019.0221>.
26. Long, B.; Zheng, W.; Schweitzer, M.; Hallen, H. Resonance Raman imagery of semi-fossilized soft tissues. *Volume*. **2018**, 10753, 1075310. <https://doi.org/10.1117/12.2321298>.
27. Casellaa, M.; Lucotti, A.; Tommasini, M.; Bedoni, M.; Forvi, E.; Gramaticac, F.; Zerbi, G. Raman and SERS recognition of  $\beta$ -carotene and haemoglobin. *Volume*. **2011**, *79*, 915–919. <https://doi.org/10.1016/j.saa.2011.03.048>.
28. Dinesh, K. R. M.; Maguire, A.; Bryant, J.; Arm-strong, J.; Dunne, M.; Finn, M.; Lyng, F. M.; Meade, A. D. Development of a high throughput (HT) Raman spectroscopy method for rapid screening of liquid blood plasma from prostate cancer patients. *The Analyst*. **2016**, *142*, 3763.
29. Wang, H.; Chen, C.; Tong, D.; Chen, C.; Gao, R.; Han, H.; Lv, X. Serum Raman spectroscopy combined with multiple algorithms for diagnosing thyroid dysfunction and chronic renal failure. *Photodiagn. Photodyn. Ther.* **2021**, *34*, 34–102241.

**Disclaimer/Publisher's Note:** The statements, opinions and data contained in all publications are solely those of the individual author(s) and contributor(s) and not of MDPI and/or the editor(s). MDPI and/or the editor(s) disclaim responsibility for any injury to people or property resulting from any ideas, methods, instructions or products referred to in the content.